Cogent Engineering

ISSN: (Print) (Online) Journal homepage: https://www.tandfonline.com/loi/oaen20

Comparative evaluation of the oxidation resistance of untreated, annealed and quenched 434 ferritic stainless steels in corrosive electrolytes

Roland Tolulope Loto |

To cite this article: Roland Tolulope Loto | (2022) Comparative evaluation of the oxidation resistance of untreated, annealed and quenched 434 ferritic stainless steels in corrosive electrolytes, Cogent Engineering, 9:1, 2045675, DOI: 10.1080/23311916.2022.2045675

To link to this article: https://doi.org/10.1080/23311916.2022.2045675

Published online: 16 Mar 2022.

Loto, *Cogent Engineering* (2022), 9: 2045675
https://doi.org/10.1080/23311916.2022.2045675

cogent engineering

MATERIALS ENGINEERING | RESEARCH ARTICLE

Comparative evaluation of the oxidation resistance of untreated, annealed and quenched 434 ferritic stainless steels in corrosive electrolytes

Roland Tolulope Loto[1*]

Received: 01 December 2021
Accepted: 23 January 2022

*Corresponding author: Roland Tolulope Loto, Mechanical Engineering, Covenant University, Nigeria
E-mail: tolu.loto@gmail.com

Reviewing editor:
Krishnan S Raja, University of Idaho, Idaho, United States

Additional information is available at the end of the article

Abstract: The corrosion resilience of untreated, annealed and quenched 434 ferritic stainless steel (434FS) was studied in 1 M H_2SO_4 media at 0–1.75% NaCl concentration. Without the chlorides, annealed 434FS depicted the maximal corrosion rate output of 21.39 mm/y in comparison with 13.60 mm/y and 13.10 mm/y for the untreated and quenched 434FS. At 0.25% NaCl concentration, a significant decrease in the corrosion of untreated 434FS was observed (3.22 mm/y), which increased progressively with an increase in NaCl concentration till 15.44 mm/y (1.75% NaCl). Corrosion of annealed 434FS decreased to 15.37 (0.25% NaCl) and 8.44 mm/y (1.75% NaCl). Corrosion of quenched 434FS increased to 17.82 mm/y before decreasing to 8.93 mm/y at 1.75% NaCl concentration. The steels exhibited significant metastable pitting behaviour. However, the potential for metastable pitting activity decreased significantly for annealed and quenched 434FS. Annealed 434FS exhibited the widest passivation sweep outputs due to the durability of its passive film compared to untreated and quenched 434FS. An increase in NaCl concentration has a minor effect on the pitting

Roland Tolulope Loto

ABOUT THE AUTHOR

Prof. Roland Tolulope Loto is a lecturer and researcher at Covenant University. He is a proven scholar in the field of metallic corrosion prevention and control. He has over two hundred research publications. He has consistently served as a reviewer in respectable journals due to his intensive knowledge and technical expertise. Roland has undertaken a number of renowned engineering research in collaboration with research/educational institutions. His in-depth experience in research experimentation basically aimed at proffering solutions to the current depreciating effect of metallic degradation and failure in service in various engineering and industrial applications. He has a Doctorate of Technology (DTech) in Metallurgical and Materials Engineering (2014) from the Tshwane University of Technology, Pretoria, South Africa, Master's Degree (MSc) in Metallurgical and Materials Engineering (2007) from the University of Lagos, Lagos, Nigeria, and a Bachelor of Technology in Mechanical Engineering (2002) from the Ladoke Akintola University of Technology, Oyo State, Nigeria.

PUBLIC INTEREST STATEMENT

The economic impact and problems resulting from corrosion have drawn strong attention from scientists worldwide. Corrosion is a major concern in chemical processing plants, oil and gas industry, manufacturing, automobile industry, marine operations, boiler plants and power generation plants due to the considerable cost involved in the replacement of metallic parts in their various applications. The consequence often leads to plant shutdowns, breakdown of industrial equipment, reduced efficiency, industrial downtime, high maintenance cost due to the replacement of the damaged parts, wastage of valuable resources and expensive overdesign. Appropriate selection of engineering with desirable corrosion-resistant properties significantly reduces corrosion damage, thus prolonging the operational lifespan of the material and subsequently minimizing the cost of corrosion prevention.

behaviour of the non-treated and 434 steels subjected to heat treatment. Optical images of annealed 434FS exhibited the highest resistance to localized deterioration with fewer corrosion pits compared to untreated and quenched 434FS in the presence of sulphates and chlorides. At the highest chloride concentration, the surface morphology of annealed 434FS showed superficial surface degradation compared to the severe surface degradation exhibited by the untreated and quenched 434FS.

Subjects: Materials Science; Corrosion-Materials Science; Metals & Alloys; Surface Engineering-Materials Science

Keywords: steel; NaCl; pitting; corrosion; passivation; H_2SO_4

1. Introduction

Corrosion is the continuous degeneration of refined engineering materials by reason of chemical and/or electrochemical reaction with the reactive anions of their various operating environments. Marcus and Maurice (1998) and Shaw and Kelly (2006) broadly discussed this phenomenon. Topala et al. (2019) and Carvalho (2014) briefly introduced this phenomenon in their work on the formation of anticorrosive strata and thin films on metal surfaces and corrosion of copper alloys in natural seawater. Research by Mehmeti and Berisha (2017) showed that mild steel reacted with SO_4^{2-} anions in an aqueous H_2SO_4 environment. Souza et al. (2015) discussed the tribo-corrosion behaviour of titanium in the oral environment and established the irreversible change of the metal resulting from the dual action of chemical, mechanical and electrochemical reactions with respect to relative contact movement. Industrial conditions, manufacturing plants, refineries and chemical processing plants are laden with different highly reactive corrosive species which aggressively react with stainless steels. Stainless steels are industrially important alloys containing a minimum of 10.5% Cr. The exceptional mechanical and corrosion-resistant attributes of stainless steels compared to carbon steel enable their broad utilization across most industries. The corrosion resilience of metallic alloys occurs is on account of the evolution of Cr_2O_3 on their surface. The oxide is passive, inert and reforms when scratched. It shields stainless steels from the harmful effect of corrosive species. However, under certain conditions, stainless steels undergo localized degeneration due to region-specific breakage of the protective covering on the steel surface. Boillot and Peultier (2014) showed that the materials section is of utmost importance in stainless steel application in industry. According to Taban et al. (2016), the properties and weldability of super martensitic stainless steels influence their corrosion behaviour. Mahato et al. (2019) showed in their study that the prolonged effect of Ti-Si-B-C nanocomposite coating 304 stainless steel in salt solution influences its localized corrosion resistance. The localized corrosion resistance of metallic alloys subjected to corrosive conditions in industrial environments was studied by other authors, which establishes that metallic alloys undergo localized deterioration differently after the collapse of their protective oxide (Kim et al., 2018; Reddy et al., 2013; Rose, 2011; Xiao et al., 2013). Corrosion of stainless steels in specific industrial environments such as crude distillation overhead systems, exhaust manifolds, desalination plants, heating reactors, production of polysilicon, etc. necessitates appropriate material selection for optimum utilization and extended operational life span of the steels. High-temperature conditions exacerbate the agitation of molecular species within an aqueous industrial environment (SO_4^{2-}, Cl^-, etc.), causing the formation of oxides, carbides, sulfides, etc. and accelerated corrosion of the steel. The consequence of the reaction mechanisms causes weakening of the metallic structure, decrease in structural integrity, breakdown of metallic properties and decrease in reliability. Hence, the need for proper material selection tailored for specific industrial requirements (Bahadori, 2014). The microstructural ability of stainless steels to remain resilient against corrosive anions in high-temperature applications is very important with respect to the weight composition of important alloying elements. This also informs further study on the protective oxide on stainless steels to understand the mechanism of passive film breakdown and repassivation. Baer (1981) studied the parameters responsible for the evolution of protective oxides on 304 stainless steel in a vacuum

chamber, while Seyeuxa et al. (2015) studied the degradation of passive film of stainless steel in the presence of bacteria. Both authors discovered that the resilience of the passive film to corrosion is significantly influenced by external factors. High-temperature applications also significantly influence the passive film characteristics of stainless steels. Previous research by the author shows that a hot aqueous environment increases the entropy and agitation of corrosive anions, which rapidly destroys the passive film of stainless steels at certain threshold chloride and temperature conditions (Loto, 2018; Loto & Loto, 2018). Under these conditions, localized destruction such as pitting is prevalent. According to Silva et al. (2021), Mollapour and Poursaeidi (2021), Pao et al. (2021), Mollapour and Poursaeidi (2021) and Zhang et al. (2022), pitting resistance and pit propagation of steels is a product of several factors related to industrial operating conditions and metallurgical propagates of the steel. Localized degradation of stainless steels can be substantially reduced with the use of modified stainless steels that remain resilient under such conditions. Heat treatment processes significantly influence the corrosion resistance of metallic alloys due to microstructural rearrangement of their metallurgical structure. High-temperature application of stainless steels are prevalent in aerospace industries, automobile exhaust mufflers, heat exchangers, boilers, etc. Usually, the application is done in an environment where stainless steels interact with corrosive anions, which invariably influences their corrosion resistance and industrial viability. The influence of annealing, normalizing and quenching heat treatment on the corrosion behaviour of API 5 L X65 pipeline steel in an acetic acid and CO_2 environment was studied. The results showed that annealed API 5 L X65 showed the lowest corrosion rate and the quenched sample displayed the highest value (Adnan et al. 2018). The effect of the heat treatment on the corrosion resistance of duplex stainless steels after isothermal ageing in the critical temperature range 750–900°C was studied by Pezzato et al. (2018). The results showed that secondary phases precipitation mainly influenced the resistance to corrosion of the lean duplex grades. Al-Quran (2010) studied the effect of intermediate annealing on the corrosion resistance of chromium_nickel steel. Observations showed an increase in the corrosion resistance of the material mainly due to the spheroidal annealing process. The effect of temperature and time of annealing on hardness indicates that the best time and temperature for corrosion is 740°C over 45 min for corrosion resistance. The corrosion resistance of E34 microalloy steel was studied in 3.5% NaCl solution in rolled and repeated quenched conditions. The results showed that with repetitive recrystallization, grains become finer, and corrosion rate increases (Seikh, 2013). Li et al. (2020) researched into the effect of annealing in the heat treatment process at 700°C on the corrosion resistance of a stainless/carbon steel bimetal plate. The higher carbon content on the carbon steel enhanced the corrosion resistance of the steel compared to the stainless steel. Fedorov et al. (2021) studied the effect of quenching temperature on the pitting corrosion resistance of lean duplex stainless steel. Observations showed that as the temperature rises, the pitting potential increases significantly due to the achievement of a favourable phase ratio. Bosing et al. (2019) studied the influence of heat treatment on the microstructure and corrosion resistance of X46Cr13 martensitic stainless steel. The results show a strong dependency of the corrosion behaviour on the heat treatment where the governing corrosion mechanism is affected differently. Quan et al. (2021) investigated the effect of temperature on the corrosion of Q235 and 16Mn steel in sodium aluminate solution. The results indicate that the corrosion rates of two steels increased with temperature. Sabzi et al. (2019) studied the effect of temperature on the corrosion behaviour of galvanized steel in the seawater environment. An increase in ambient temperature results in higher corrosion current densities. In contribution to the research of heat treatment effect and high-temperature variation on the corrosion resistance of metallic alloys, this manuscript studies the consequence of high temperature on the deterioration resilience of 434 ferritic stainless steels in low-concentration electrolytes.

2. Experimental methods

434 ferritic stainless steel (434FS) with average elemental constituents (wt. %) depicted in Table 1 was sliced into 15 test specimens with median surface dimensions of 0.81 cm^2. The steel samples were divided into three different categories (untreated, quenched and annealed 434FS) of five 434FS specimens each. The annealing and quenching heat-treatment process of 434FS was carried out within an

Table 1. Constituents (wt. %) of 434FS

Element	P	S	C	Cr	Ni	Cu	Mn	Si	Fe
% Content	0.041	0.029	0.15	16	0.36	0.3	1.1	1.2	80.82

open furnace wherewith the steel was heated to 700°C and sustained for 30 min. Annealed 434FS specimens were cooled in atmospheric air, whereas the quenched 434FS specimens were cooled in deionized H_2O. The temperature of the furnace was controlled to an accuracy of ±10°C and coupled to a K-model thermocouple. The 434FS samples were then placed in semi-hardened acrylic mixture, which was smoothened with abrasive cloth with grits of 120, 220, 320, 600, 800 and 1,000. Burnishing of the sample surface was done with diamond fluid. A 200 mL volumetric value of 1 M H_2SO_4 was produced in five separate formats from standard quality H_2SO_4 fluid (98%). The acid was mixed with NaCl at 0%, 0.25%, 0.75%, 1.25% and 1.75% NaCl concentrations. Potentiostatic evaluation was undertaken with a triple cord electrode inside a transparent receptacle containing 300 mL of the H_2SO_4–NaCl media and plugged to a Digi-Ivy measuring instrument. Potentiodynamic polarization charts were plotted at inspection counts of 0.0015 V/s (−0.85 V to +1.85 V). Corrosion current I_D (A), corrosion current density J_D (A/cm^2) and corrosion potential C_P (V) data were extracted from Tafel plots. The corrosion rate, C_R (mm/y), was evaluated as follows

$$C_R = \frac{0.00327 \times C_D \times E_Q}{D} \tag{1}$$

E_Q illustrates the corresponding weight (g) of 434FS, 0.00327 indicates the constant relating to the corrosion rate and D depicts density (g). Open circuit potential evaluation of 434FS was carried out at a step potential of 0.1 V/s (5400 s) with a Digi-Ivy 2311 device. Optical microscopic characterization was performed on the steel surface with the use of a metallurgical microscope.

3. Results and discussion

3.1. Open circuit potential evaluation

Open circuit potential illustrative plots for untreated, annealed and quenched 434FS in 1 M H_2SO_4 media at 0%, 0.25% and 1.75% NaCl concentrations are shown in Figure 1(a–c). The plots for the untreated steel initiated at −0.460 V, −0.449 V and −0.442 V (0%, 0.25% and 1.75% NaCl concentrations) and steeply decreased to −0.464 V, −0.464 V and −0.457 V at 300s before progressively increasing to −0.450 V, −0.450 V and −0.443 V at 3600 s. Plot configurations show that the plot at 2% NaCl concentration demonstrated the most electropositive transition signifying higher resilience of the passive on 434FS, while the plots at 0% and 0.25% NaCl concentrations displayed a similar configuration signifying limited influence of low NaCl concentration on the thermodynamic behaviour of untreated 434FS. The open-circuit potential plot configurations for annealed and quenched 434FS were generally similar, with the plots at 0% NaCl configuration being highly electropositive due to the strength of its inert oxide. The plots at 0% NaCl concentration for the annealed and quenched 434FS commenced at 0.08 V and −0.014 V and culminated at 0.091 V and 0.089 V (3600 s). At 0.25% and 1.75% NaCl concentrations, the plot configuration for the annealed steel commenced at −0.454 V and −0.429 V and culminated at −0.447 V and −0.419 V. The corresponding values for the quenched steel commenced at −0.463 V and −0.446 V and culminated at −0.448 V and −0.422 V (3600 s). In general, the plot configurations of the annealed and quenched 434FS at 0.25% and 1.75% NaCl concentrations show that heat treatment increases the thermodynamic proclivity of the heat-treated steel to degrade in the presence of chlorides compared to the untreated steel where high chloride concentration induces a more resilient passive film of the steel.

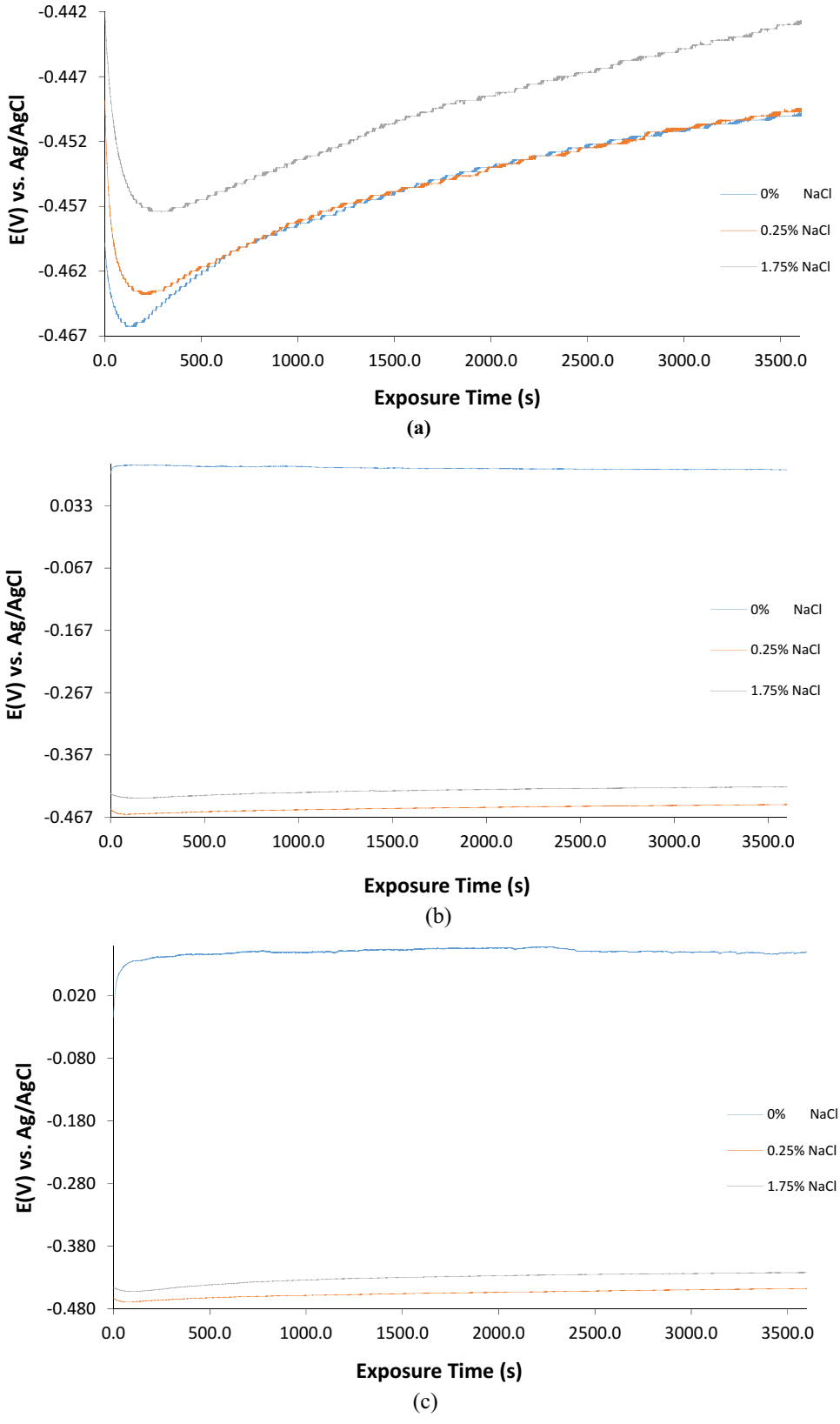

Figure 1. Open circuit potential plots for 434FS in 1 M H_2SO_4 media at 0%, 0.25% and 1.75% NaCl concentrations: (a) untreated steel, (b) annealed steel and (c) quenched steel.

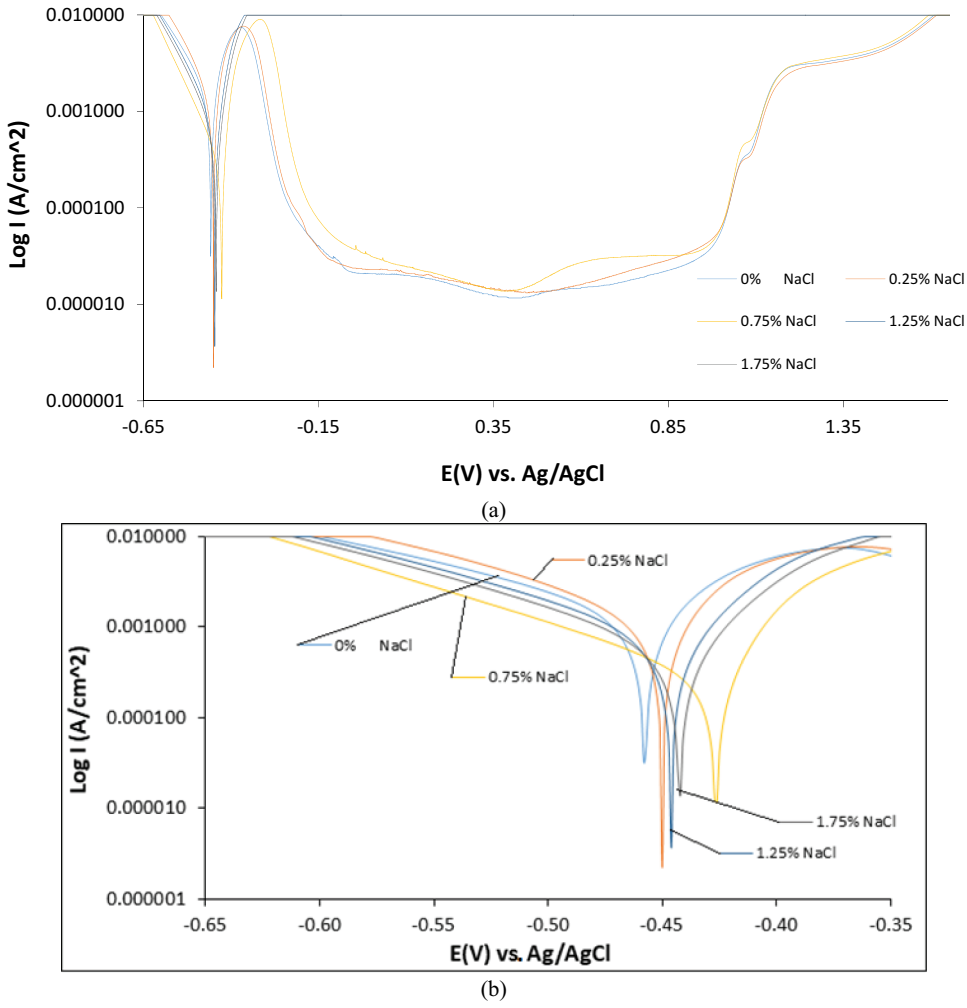

Figure 2. Potentiodynamic polarization data for (a) untreated 434FS in 1 M H_2SO_4 media at 0% to 1.75% NaCl solution and (b) close-up view of the untreated 434FS polarization plots.

3.2. Potentiodynamic polarization studies

Potentiodynamic polarization plots for untreated, annealed and quenched 434FS with respect to NaCl concentration in 1 M H_2SO_4 electrolyte are shown in Figures 2(a)–4(b). The results retrieved from the polarization plots are presented in Table 2. The results for untreated 434FS show that NaCl concentration influences the corrosion behaviour of the steel. The corrosion output of untreated 434FS is 13.60 mm/y at 0% NaCl, which corresponds to the corrosion current density of 1.25×10^{-3} A/cm^2. The rate of degradation decreased drastically to 3.22 mm/y at 0.25% NaCl concentration, signifying increased resistance of untreated 434FS to corrosion within the vicinity of low chloride concentration. This occurs owing to the growth of an unreactive protective covering on the steel exterior from the reaction of dissolved O_2 with Cr (Cr_2O_3). The protective oxide hinders the adsorption and reaction of the chlorides with the steel due to the stability and growth of the oxide through a solid-state growth process, according to Duan et al. (2016). An increase in NaCl concentration to 0.75% concentration results in adsorption and reaction of limited chloride anions with the steel, resulting in a corrosion rate of 9.49 mm/y. Parangusan et al. (2021) showed in their work that an increase in Cl ion concentration results in an oscillation within the oxygen evolution region, causing the collapse of the passive layer and pit initiation. The relatively smaller size of Cl ions and high reactivity enable unrestricted diffusion of miniature breakage of the protective film at regions of flaws, impurities and inclusions. Steady addition to NaCl concentration correlates with an increase in the corrosion output till 15. 44 mm/y at 1.75% NaCl concentration. Corrosion rate results obtained for annealed 434FS significantly differ from untreated 434FS. In 0% NaCl

Table 2. Potentiodynamic polarization output for untreated, annealed and quenched 434FS in 1 M H_2SO_4 media at 0% to 1.75% NaCl solution

Untreated 434FS								
Sample	**NaCl Conc. (%)**	**C_R (mm/y)**	**434FS I_D (A)**	**J_D (A/cm^2)**	**C_P (V)**	**Pol. Res., R_p (Ω)**	**Cath. Tafel Slope, B_c (V/dec)**	**Anod. Tafel Slope, B_a (V/dec)**
A	0	13.60	1.01E-03	1.25E-03	−0.462	25.37	−6.611	2.957
B	0.25	3.22	2.40E-04	2.96E-04	−0.450	68.69	−7.264	3.246
D	0.75	9.49	7.07E-04	8.72E-04	−0.436	40.37	−8.082	6.468
F	1.25	16.19	1.21E-03	1.49E-03	−0.446	16.30	−7.327	6.468
H	1.75	15.44	1.15E-03	1.42E-03	−0.442	18.48	−7.781	8.351
Annealed 434FS								
Sample	**NaCl Conc. (%)**	**C_R (mm/y)**	**434FS I_D (A)**	**J_D(A/cm^2)**	**C_P (V)**	**Pol. Res., R_p (Ω)**	**Cath. Tafel Slope, B_c (V/dec)**	**Anod. Tafel Slope, B_a (V/dec)**
A	0	21.39	1.59E-03	1.97E-03	−0.446	16.13	−6.770	3.387
B	0.25	15.37	1.15E-03	1.41E-03	−0.445	22.43	−7.306	5.162
D	0.75	13.96	1.04E-03	1.28E-03	−0.448	24.69	−7.371	6.629
F	1.25	11.66	8.69E-04	1.07E-03	−0.438	29.57	−5.964	6.693
H	1.75	8.44	6.29E-04	7.76E-04	−0.448	40.86	−8.117	9.198
Quenched 434FS								
Sample	**NaCl Conc. (%)**	**C_R (mm/y)**	**434FS I_D (A)**	**J_D(A/cm^2)**	**C_P (V)**	**Pol. Res., R_p (Ω)**	**Cath. Tafel Slope, B_c (V/dec)**	**Anod. Tafel Slope, B_a (V/dec)**
A	0	13.10	9.76E-04	1.20E-03	−0.454	26.33	−6.270	3.395
B	0.25	17.82	1.33E-03	1.64E-03	−0.448	19.36	−8.239	4.185
D	0.75	15.76	1.17E-03	1.45E-03	−0.450	21.89	−6.839	6.843
F	1.25	8.58	6.39E-04	7.89E-04	−0.444	40.20	−8.417	9.471
H	1.75	8.93	6.65E-04	8.21E-04	−0.435	38.58	−6.929	11.840

cogent engineering

Table 3. Potentiostatic data for untreated, annealed and quenched 434FS in 1 M H_2SO_4 at a specific NaCl concentration

Untreated 434FS							
NaCl Conc. (%)	**M_P V (V)**	**M_P I (A)**	**P_P (V)**	**Pass. I (A)**	**Pass. Range (V)**	**Pit V (V)**	**Pit I (A)**
0	−0.36	0.0072	−0.11	3.03E−05	1.09	0.98	4.08E−05
0.25	−0.37	0.0076	−0.12	2.91E−05	1.10	0.98	5.72E−05
0.75	−0.32	0.0090	−0.10	4.87E−05	1.06	0.96	4.81E−05
Annealed 434FS							
NaCl Conc. (%)	**M_P V (V)**	**M_P I (A)**	**P_P (V)**	**Pass. I (A)**	**Pass. Range (V)**	**Pit V (V)**	**Pit I (A)**
0	−0.36	0.0071	−0.06	1.76E−05	0.99	0.93	5.50E−05
0.25	−0.30	0.0098	−0.08	3.34E−05	1.11	1.03	0.00023
0.75	−0.32	0.0085	−0.15	8.82E−05	1.17	1.02	0.00022
1.25	−0.16	0.0087	−0.13	0.00017	1.24	1.11	0.0022
Quenched 434FS							
NaCl Conc. (%)	**M_P V (V)**	**M_P I (A)**	**P_P (V)**	**Pass. I (A)**	**Pass. Range (V)**	**Pit V (V)**	**Pit I (A)**
0	−0.36	0.0668	−0.17	8.39E−05	1.18	1.01	0.00012
0.25	−0.34	0.0086	−0.15	8.62E−05	1.15	1.00	7.01E−05
0.75	−0.04	0.0099	−0.01	0.00017	1.00	0.99	7.84E−05

concentration, the annealed 434FS corrosion value is 21.39 mm/y, making it substantially higher

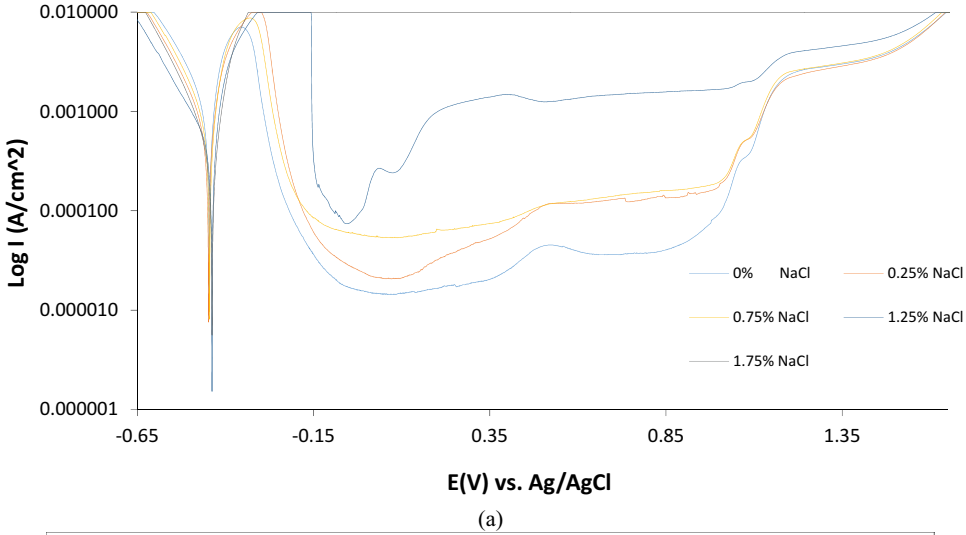

(a)

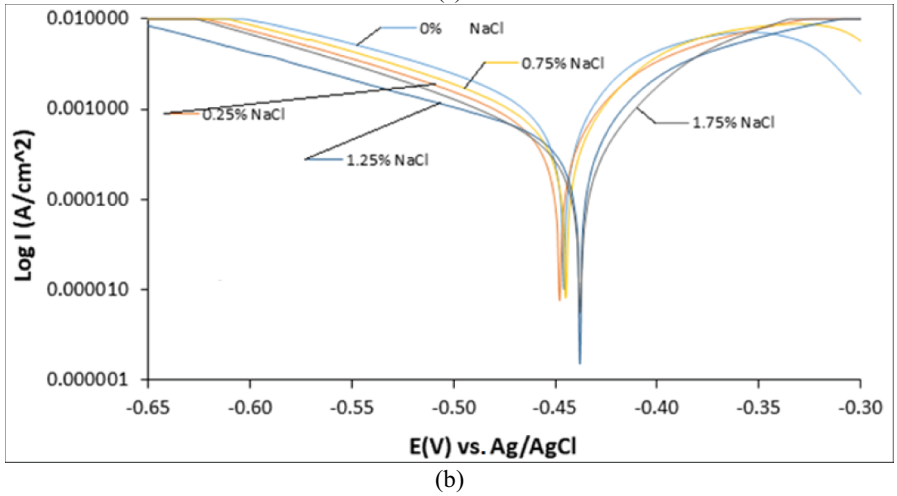

(b)

Figure 3. Potentiodynamic polarization data for (a) annealed 434FS in 1 M H_2SO_4 media at 0% to 1.75% NaCl solution and (b) close-up view of the annealed 434FS polarization plots.

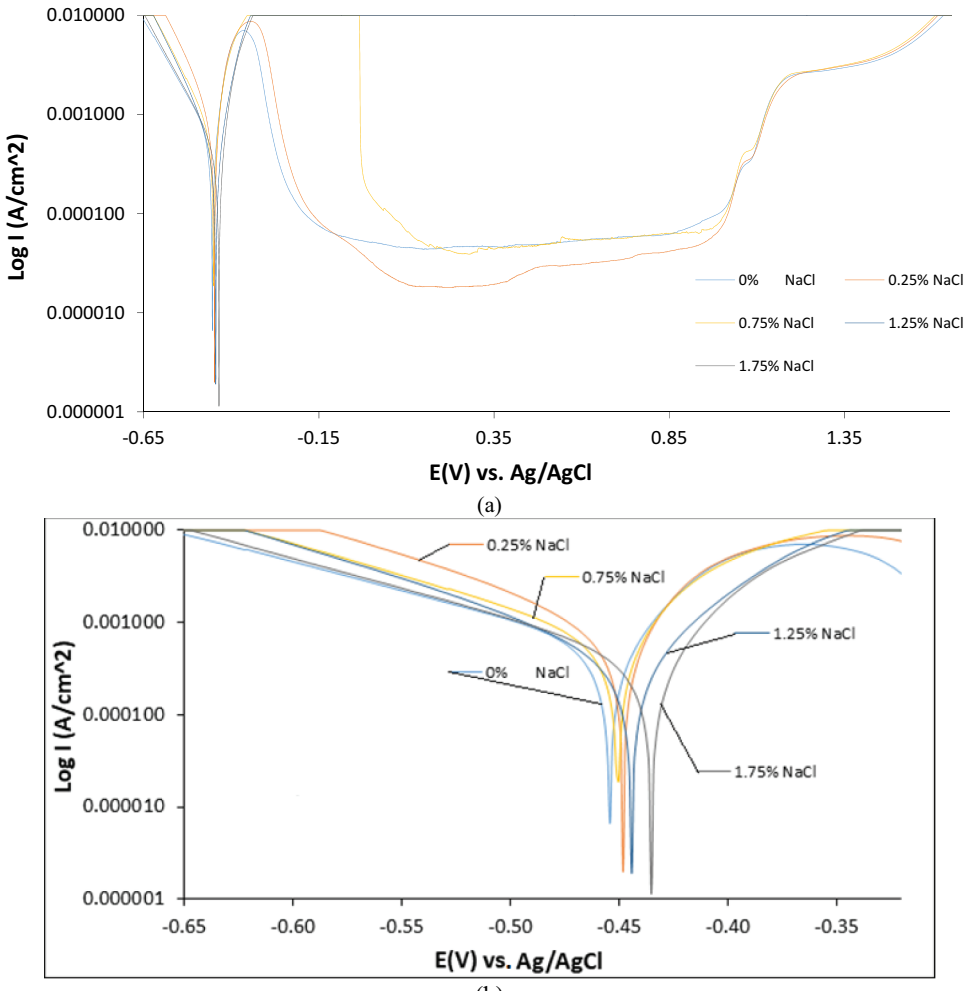

Figure 4. Potentiodynamic polarization data for (a) quenched 434FS in 1 M H_2SO_4 media at 0% to 1.75% NaCl solution and (b) close-up view of the quenched 434FS polarization plots.

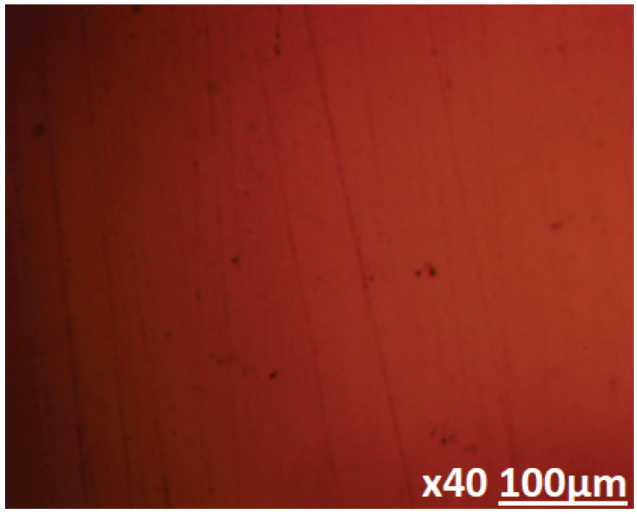

Figure 5. Optical illustration of 434FS prior to corrosion test.

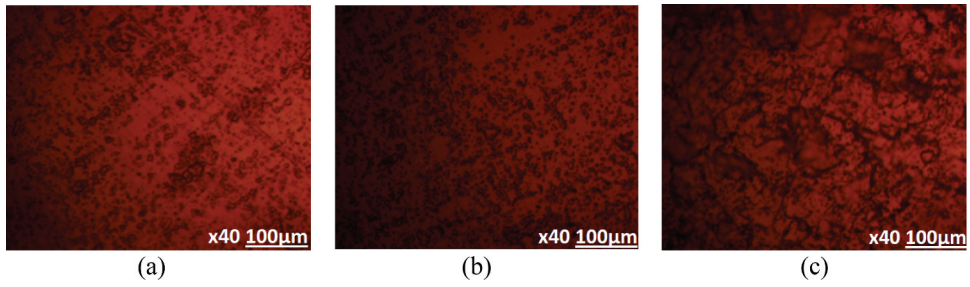

Figure 6. Optical illustrations of untreated 434FS following corrosion in 1 M H_2SO_4 electrolyte at (a) 0% NaCl concentration, (b) 0.25% NaCl concentration and (c) 1.75% NaCl concentration.

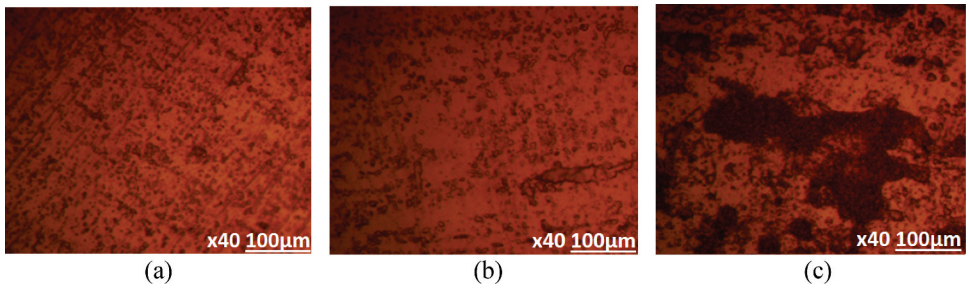

Figure 7. Optical illustrations of annealed 434FS following corrosion in 1 M H_2SO_4 electrolyte at (a) 0% NaCl concentration, (b) 0.25% NaCl concentration and (c) 1.75% NaCl concentration.

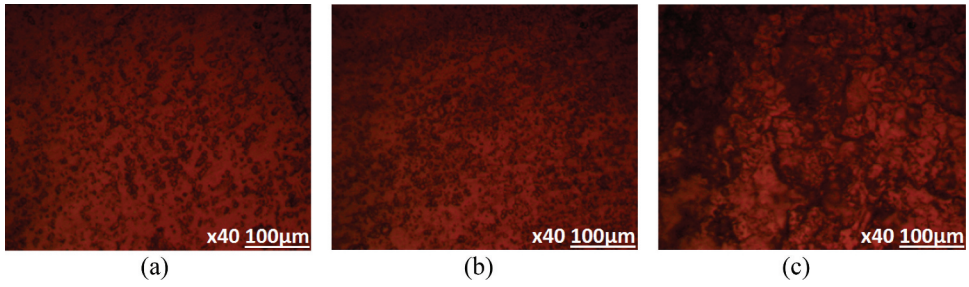

Figure 8. Optical illustrations of quenched 434FS following corrosion in 1 M H_2SO_4 media at (a) 0% NaCl concentration, (b) 0.25% NaCl concentration and (c) 1.75% NaCl concentration.

than the related output obtained for untreated 434FS (13.60 mm/y) due to significant alteration of the metallurgical structure of 434FS. However, addition to NaCl concentration causes a proportionate decline in the corrosion rate of annealed 434FS till 8.34 mm/y at 1.75% NaCl concentration which directly relates to J_D of 6.29 × 10^{-4} A/cm^2. The rate of degradation of quenched 434FS was generally high and comparable to the results obtained for annealed 434FS at low NaCl concentration 0–0.75% NaCl concentration. After 0.75% NaCl concentration, the corrosion output of quenched 434FS was generally smaller than the data retrieved for untreated and annealed 434FS. The results show that heat treatment improves the corrosion resilience of 434FS at higher NaCl concentrations compared to untreated 434FS. However, quenching heat treatment imparts the highest general corrosion resistance to 434FS with corrosion rate outputs averagely smaller than the outputs obtained for the untreated and annealed 434FS. The high cathodic and anodic Tafel slope values are due to their low exchange current densities at equilibrium potential. The exchange current density indicates the rate of oxidation and reduction reactions at the metal electrode. The lower the exchange current density, the slower the redox electrochemical reaction. Hence, the values in the manuscript tables show that the presence of the inhibitors significantly reduced the oxidation half-cell reactions compared to the cathodic

counterpart. While the values may be generally high, it is due to hysteresis in electrochemical reactions at molecular and atomic levels, which invariably are strongly dependent on the composition of the metal/alloy the acid solution, the concentration of the soluble species.

3.3. Potentiostatic studies

Potentiostatic data of the pitting and passivation attributes of untreated, annealed and quenched 434FS from Figures 2 (a)–4(b) are shown in Table 3. The metastable pitting (M_P) region of the polarization plot immediately follows anodic polarization. It is the portion where transient corrosion pits initiate, propagate and eventually collapse at the onset of passivation of the steel. The metastable region reveals the ability of the steel to quickly passivate after anodic dissolution reactions. Generally, metastable pitting initiates at higher potentials with an increase in NaCl concentration. Untreated 434FS displays the widest metastable pitting region before passivation of the steel, while annealed 434FS exhibited a significant decrease in metastable pitting portion analogous to an increase in NaCl concentration. The metastable pitting region of quenched 434FS was comparable to untreated 434FS with the exception of delayed metastable pitting activity at 0.75% NaCl concentration. The passivation potential (P_P) is the potential and region of the polarization plot where metastable transient pits collapse and the evolution of a protective barrier on the steel is stable during potential scanning. The passivation potential for untreated, annealed and quenched 434FS varies significantly with respect to NaCl concentration. Passivation behaviour initiated earlier for quenched 434FS at 0% and 0.25% NaCl concentrations compared to the output obtained for untreated and annealed 434FS. Though annealed 434FS showed the second-highest output at 0.75% and 1.25% NaCl concentrations. The value for extent of passivation shows the resilience of the passive protective covering on 434FS. The highest passivation range value of 1.24 V was obtained for quenched 434FS at 1.25% NaCl concentration signifying higher resistance to localized corrosion deterioration. Variation in pitting (Pit) potential values shows that NaCl concentration has a curbed effect on the pitting resistance of untreated, annealed and quenched 434FS though pitting potential values show that annealed 434FS exhibited the higher pitting corrosion resistance.

3.4. Optical microscopy analysis

Optical illustrations of 434FS preceding corrosion and images after corrosion (untreated, annealed and quenched) of 434FS in 1 M H_2SO_4 (0%, 0.25% and 1.75% NaCl) concentration are illustrated in Figure 5, Figure 6 (a–c), Figure 7 (a–c) and Figure 8 (a–c). Figure 5 illustrates the image of 434FS before corrosion after the metallographic test. The optical images of untreated, annealed and quenched 434FS following corrosion in 1 M H_2SO_4 at 0% and 0.25% NaCl [Figure 6 (a) to 8(b)] depicts the presence of numerous corrosion pits. However, the corrosion pits on the untreated and quenched 434FS [Figure 6 (a) and Figure 8 (a)] at 0% NaCl concentration are generally larger than the pits on the annealed steel [Figure 7 (a)]. The pits on the annealed steel are generally smaller and fewer by reason of the greater resilience of the annealed steel to localized deterioration. At 0.25% NaCl concentration, a similar observation was determined with the corrosion pits on the untreated and quenched steel [Figure 6 (b) and Figure 8 (b)] were significantly more numerous than the observation for the annealed steel [Figure 7 (b)] for reasons earlier mentioned. The optical images of untreated, annealed and quenched 434FS [Figures 6 (c)–8(c) at 1.75% NaCl showed more severe surface deterioration by reason of the presence of higher concentration of Cl^-. However, the surface deterioration of the annealed steel tends to be superficial compared to that of the untreated and quenched steel.

4. Conclusion

Corrosion of untreated, annealed and quenched 434 ferritic stainless steel was studied in low concentration sulphate-chloride solution. The following conclusions were reached.

- The annealed steel depicts the optimal general resistance to corrosion with corrosion rate outputs decreasing with an increment in chloride concentration.

- Annealed ferritic steel also revealed the highest resistance to localized corrosion with its passivation range values rising with an upsurge in chloride concentration due to the durability of its inert oxide in comparison to the untreated and quenched ferritic steel.
- Optical illustrations of the annealed steel exterior revealed the presence of scanty corrosion pits and less degraded surface morphology compared to the untreated and quenched steel surfaces.
- Open circuit potential plots demonstrate that heat treatment surges the thermodynamic proclivity of 434 steel to corrode despite improved general resilience to corrosion in correlation to the untreated steel.

Acknowledgements
The author recognizes the financial support of Covenant University and the provision of facilities towards the actualization of this research.

Funding
The author received no direct funding for this research.

Author details
Roland Tolulope Loto[1]
E-mail: tolu.loto@gmail.com
ORCID ID: http://orcid.org/0000-0002-1675-8989
[1] Department of Mechanical Engineering, Covenant AQ2 University, Ota, Nigeria.

Disclosure statement
No potential conflict of interest was reported by the author(s).

Citation information
Cite this article as: Comparative evaluation of the oxidation resistance of untreated, annealed and quenched 434 ferritic stainless steels in corrosive electrolytes, Roland Tolulope Loto, *Cogent Engineering* (2022), 9: 2045675.

References

A-Itawi, H.I., & Al-Quran, F., (2010). Effects of annealing and annealing cooling media in corrosion resistance and microhardness of low content chromium nickel steel. Advances in Theoretical and Advance Mechanics, 3(2), 89–97.

Adnan, M. A., Kee, K.-E., Raja, P. B., Ismail, M. C., & Kakooei, S. (2018). Influence of heat treatment on the corrosion of carbon steel in environment containing carbon dioxide and acetic acid. *IOP Conference Series: Materials Science and Engineering*, *370*, 012039. https://doi.org/10.1088/1757-899X/370/1/012039

Baer, D. R. (1981). Protective and non-protective oxide formation on 304 stainless steel. *Applied Surface Science*, *7*(1–2), 69–82. https://doi.org/10.1016/0378-5963(81)90061-1

Bahadori, A. (2014). *Corrosion and materials selection: A guide for the chemical and petroleum industries*. John Wiley & Sons Ltd. https://doi.org/10.1002/9781118869215

Boillot, P., & Peultier, J. (2014). Use of stainless steels in the industry: Recent and future developments. *Procedia Engineering*, *83*, 309–321. https://doi.org/10.1016/j.proeng.2014.09.015

Bösing, I., Cramer, L., Steinbacher, M., Zoch, H. W., Thöming, J. T., & Baune, M. (2019). Influence of heat treatment on the microstructure and corrosion resistance of martensitic stainless steel. *AIP Advances*, *9*(6), 065317. https://doi.org/10.1063/1.5094615

Carvalho, M. L., (2014). *Corrosion of copper alloys in natural seawater: Effects of hydrodynamics and pH*. Analytical chemistry. Université Pierre et Marie Curie – Paris. https://tel.archives-ouvertes.fr/tel-01207012/document

Duan, Z., Arjmand, F., Zhang, L., & Abe, H. (2016). Investigation of the corrosion behavior of 304L and 316L stainless steels at high-temperature borated and lithiated water. *Journal of Nuclear Science and Technology*, *53*(9), 1435–1446. https://doi.org/10.1080/00223131.2015.1125311

Fedorov, A., Zhitenev, A., & Strekalovskaya, D., 2021. Effect of heat treatment on the microstructure and corrosion properties of cast duplex stainless steels. *E3S Web of Conferences* St. Petersburg, Russia, 225, 01003. https://doi.org/10.1051/e3sconf/202122501003.

Kim, S. I., Lee, H. Y., & Song, J. S. (2018). A study on characteristics and internal exposure evaluation of radioactive aerosols during stainless pipe cutting in decommissioning of nuclear power plant. *Nuclear Engineering and Technology*, *50*(7), 1088–1098. https://doi.org/10.1016/j.net.2018.06.010

Li, H., Zhang, L., Zhang, B., & Zhang, Q. (2020). Effect of heat treatment on the microstructure and corrosion resistance of stainless/carbon steel bimetal plate. *Advances in Materials Science and Engineering*, 1280761. https://doi.org/10.1155/2020/1280761

Loto, R. T. (2018). Effect of elevated temperature on the corrosion polarization of NO7718 and NO7208 nickel alloys in hot acid chloride solution. *Journal of Bio- and Tribo-Corrosion*, *4*(4), 71. https://doi.org/10.1007/s40735-018-0190-8

Loto, R. T., & Loto, C. A. (2018). Corrosion behaviour of S43035 ferritic stainless steel in hot sulphate/chloride solution. *Journal of Materials Research Technology*, *7*(3), 231–239. https://doi.org/10.1016/j.jmrt.2017.07.004

Mahato, P., Mishra, S. K., Murmu, M., Murmu, N. C., Hirani, H., & Banerjee, P. (2019). A prolonged exposure of Ti-Si-B-C nanocomposite coating in 3.5 wt% NaCl solution: Electrochemical and morphological analysis. *Surface & Coatings Technology*, *375*, 477–488. https://doi.org/10.1016/j.surfcoat.2019.07.039

Marcus, P., & Maurice, V. 1998. Fundamental aspects of corrosion of metallic materials. In *Materials Science and Engineering* (Vol. II, pp. 1–34). EOLSS Publishers Co. Ltd.

Mehmeti, V. V., & Berisha, A. V. (2017). Corrosion Study of mild steel in aqueous sulfuric acid solution using 4-Methyl-4H-1,2,4-Triazole-3-Thiol and 2-Mercaptonicotinic Acid—An experimental and Theoretical Study. *Frontiers in Chemistry*, *5*. https://doi.org/10.3389/fchem.2017.00061

Mollapour, Y., & Poursaeidi, E. (2021). Experimental and numerical analysis of pitting corrosion in CUSTOM 450 stainless steel. *Engineering Failure Analysis*, *128*, 105589. https://doi.org/10.1016/j.engfailanal.2021.105589

Pao, L., Muto, I., & Sugawara, Y. (2021). Pitting at inclusions of the equiatomic CoCrFeMnNi alloy and improving corrosion resistance by potentiodynamic polarization in H_2SO_4. *Corrosion Science*, *191*, 109748. https://doi.org/10.1016/j.corsci.2021.109748

Parangusan, H., Bhadra, J., & Al-Thani, N. (2021). A review of passivity breakdown on metal surfaces: Influence of chloride- and sulfide-ion concentrations, temperature, and pH. *Emergent Materials*, *4*(5), 1187–1203. https://doi.org/10.1007/s42247-021-00194-6

Pezzato, L., Lago, M., Brunelli, K., Breda, M., & Irene Calliari, I. (2018). Effect of the heat treatment on the corrosion resistance of duplex stainless steels. *Journal of Materials Engineering and Performance*, *27*(8), 3859–3868. https://doi.org/10.1007/s11665-018-3408-5

Quan, B., Li, J., & Chen, C. (2021). Effect of corrosion temperature on the corrosion of Q235 steel and 16Mn steel in sodium aluminate solutions. *ACS Omega*, *6*(40), 25904–25915. https://doi.org/10.1021/acsomega.1c02220

Reddy, V. S., Kaushik, S. C., Ranjan, K. R., & Tyagi, S. K. (2013). State-of-the-art of solar thermal power plants—A review. *Renewable and Sustainable Energy Reviews*, *27*, 258–273. https://doi.org/10.1016/j.rser.2013.06.037

Rose, R. (2011). *On the degradation of porous stainless steel*. University of British Columbia.

Sabzi, M., Dezfuli, S. M., Asadian, M., Tafi, A., & Ali, M. (2019). Study of the effect of temperature on corrosion behavior of galvanized steel in seawater environment by using potentiodynamic polarization and EIS methods. *Materials Research Express*, *6*(7), 076508. https://doi.org/10.1088/2053-1591/ab10ad

Seikh, A. H. (2013). Influence of heat treatment on the corrosion of microalloyed steel in sodium chloride solution. *Journal of Chemistry*, *58*, 7514. https://doi.org/10.1155/2013/587514

Seyeuxa, A., Zannaa, S., Allion, A., & Marcus, P. (2015). The fate of the protective oxide film on stainless steel upon early stage growth of a biofilm. *Corrosion Science*, *91*, 352–356. https://doi.org/10.1016/j.corsci.2014.10.051

Shaw, B. A., & Kelly, R. G. (2006). What is corrosion? *Electrochemical Society Interface*, *15*(1), 24–26. https://doi.org/10.1149/2.F06061IF

Silva, R., Kugelmeier, C. L., Vacchi, G. S., Martins Junior, C. B., Dainezi, I., Afonso, C. R. M., Mendes Filho, A. A., & Roverea, C. A. D. (2021). A comprehensive study of the pitting corrosion mechanism of lean duplex stainless steel grade 2404 aged at 475 °C. *Corrosion Science*, *191*, 109738. https://doi.org/10.1016/j.corsci.2021.109738

Souza, J. C. M., Henriques, M., Teughels, W., Ponthiaux, P., Celis, J. P., & Rocha, L. A. (2015). Wear and corrosion interactions on titanium in oral environment: Literature review. *Journal of Bio and Tribo Corrosion*, *1*(13). http://dx.doi.org/10.1007/s40735-015-0013-0

Taban, E., Kaluc, E., & Ojo, O. O. (2016). Properties, weldability and corrosion behavior of supermartensitic stainless steels for on- and offshore applications. *MP Materials Testing*, *58*(6), 501–518. https://doi.org/10.3139/120.110884

Topala, P., Ojegov, A., & Besliu, V. (2019). *Formation of anticorrosive structures and thin films on metal surfaces by applying EDM*. IntechOpen. http://dx.doi.org/10.5772/intechopen.80543

Xiao, G., Wang, X., Zhang, J., Ni, M., Gao, X., Luo, Z., & Cen, K. (2013). Granular bed filter: A promising technology for hot gas clean-up. *Powder Technology*, *244*, 93–99. https://doi.org/10.1016/j.powtec.2013.04.003

Zhang, X., Zhao, S., Wang, Z., Li, J., & Qiao, L. (2022). The pitting to uniform corrosion evolution process promoted by large inclusions in mooring chain steels. *Materials Characterization*, *181*, 111456. https://doi.org/10.1016/j.matchar.2021.111456

***Cogent Engineering* (ISSN: 2331-1916) is published by Cogent OA, part of Taylor & Francis Group.**